CSI-SF: Estimating Wireless Channel State Using CSI Sampling & Fusion

Riccardo Crepaldi*, Jeongkeun Lee†, Raul Etkin†, Sung-Ju Lee†, Robin Kravets*
*University of Illinois at Urbana-Champaign
†Hewlett-Packard Laboratories
Email:{rcrepal2,rhk}@illinois.edu, {jklee,raul.etkin,sjlee}@hp.com

***Abstract*—One of the key features of high speed WLAN such as 802.11n is the use of MIMO (Multiple Input Multiple Output) antenna technology. The MIMO channel is described with fine granularity by Channel State Information (CSI) that can be utilized in many ways to improve network performance. Many complex parameters of a MIMO system require numerous samples to obtain CSI for all possible channel configurations. As a result, measuring the complete CSI space requires excessive sampling overhead and thus degrades network performance. We propose CSI-SF (CSI Sampling & Fusion), a method for estimating CSI for every MIMO configuration by sampling a small number of frames transmitted with different settings and extrapolating data for the remaining settings. For instance, we predict CSI of multi-stream settings using CSI obtained only from single stream packets. We evaluate the effectiveness of CSI-SF in various scenarios using our 802.11n testbed and show that CSI-SF provides an accurate, complete knowledge of the MIMO channel with reduced overhead from traditional sampling. We also show that CSI-SF can be applied to network algorithms such as rate adaptation, antenna selection and association control to significantly improve their performance and efficiency.**

I. Introduction

While the deployment of 802.11 WLANs (Wireless Local Area Networks) is continuously increasing, the demand for reliable high bandwidth WLANs is exploding due to the demands of applications such as HD (High Definition) video streaming. Additionally, with the increasing popularity of smartphones, Wi-Fi offloading [1] alleviates the load on low throughput cellular links, but increases the bandwidth demand for Wi-Fi.

In response to this growing demand of applications and services, the new IEEE 802.11n [2] and the emerging IEEE 802.11ac [3] standards aim to provide very high throughput WLANs by improving on the existing 802.11 standards. Some of the key enhancements used for increasing the PHY throughput are using wider, bonded channels (40 MHz in 802.11n and up to 160 MHz in 802.11ac) and MIMO (Multiple Input Multiple Output) antennas [4], [5]. Currently available 802.11n devices support up to three MIMO spatial streams.

To achieve improved performance at MAC and application layers, algorithms and protocols for WLANs now need to consider these new features offered by the use of multiple antennas. For instance, while before rate adaptation only selected the modulation and coding rate, it now needs to consider the number of concurrent spatial data streams transmitted. Essentially, optimal WLAN performance required detailed knowledge of the wireless link. Such information is available through the use of Channel State Information (CSI), which describes the current condition of the channel, and consists of the attenuation and phase shift experienced by each spatial stream to each receive antenna in each of the OFDM subcarriers. CSI is determined in the 802.11n hardware by analyzing received packets using training sequences in the packet headers. For network algorithms such as rate selection, AP association and channel assignment, timely optimal decisions require accurate CSI estimates under various settings (e.g., different number of spatial streams, transmission antennas used, transmission powers, etc.). However, some settings might not have been sampled for recently received packets and so additional frame transmissions are necessary to obtain a complete and fresh CSI. These extra transmissions consume bandwidth and increase latency, and ultimately degrade system performance if over used.

To enable the effective use of CSI, we present CSI-SF (Channel State Information with Sampling and Fusion), a CSI processing technique that predicts the CSI of non-sampled MIMO configurations, using a small number of samples. Protocols using CSI-SF can predict the CSI of a 3×3 channel using CSI measured from packets sent using a 1×3 configuration. We evaluate the accuracy of CSI-SF by comparing its CSI estimates against the actual measured channel conditions in our 802.11n testbed. We also describe the practical challenges of accurately estimating CSI and assess CSI-SF without the knowledge of hardware specific characteristics. We demonstrate how network algorithms such as rate adaptation, antenna selection, and association control can utilize CSI-SF to enhance the efficiency and hence improve network performance.

The rest of this paper is organized as follows. In Section II, we survey the related work and describe the motivations that led us to the development of CSI-SF. In Section III, we provide the analytical foundations of our technique, and in Section IV, we present results of its application in real-world traces that we collected in the evaluation of CSI-SF on our 802.11n testbed. In Section V, we discuss application uses of CSI-SF and Section VI concludes the paper.

II. Channel Quality Metric

A. Related Work

Wireless network algorithms maximize the network performance by using channel quality information to fine tune protocol configurations (e.g., modulation, coding rate, number

of streams, set of transmit antennas, transmission power, etc.). For example, many rate adaptation algorithms such as ARF [6], AARF [7] and SARA [8] probe the channels to collect statistical information at different bitrates. These probing-based schemes incur excessive messaging overhead when there is a large number of configurations to probe. Additionally, it takes long to converge, especially when the gap between the rate of the probed packets and the optimal rate is large. Moreover, optimal bitrate selection requires the differentiation of losses from wireless errors and losses from collisions/congestion [9], [10], [11].

Many algorithms take an alternative approach and use Signal to Noise Ratio (SNR) as the channel quality metric (e.g., RBAR [12]). SNR is easy to compute and is already provided by current 802.11 hardware. However, it was shown that wireless networks have complex error distributions and SNR does not well-represent channel quality [13], [14]. In particular, the authors of [15] show that SNR is not the right metric to determine achievable throughput, in large part due to the fact that the frequency selectivity of the wideband 802.11 channel is not captured by SNR. Moreover, in OFDM modulation, subcarriers with a low SNR have a stronger effect on the overall probability of error.

Recent standards such as IEEE 802.11n [2] and 802.11ac [3] utilize MIMO transceivers [4], [5], which increase the degrees of freedom and so the complexity of rate selection. Essentially, along with selecting modulation and coding schemes, rate selection algorithms must now choose the correct number of concurrent data streams. Optimizations can be based on the CSI read from the 802.11 hardware. In [16], [15], [17], the detailed information in the CSI report is used to determine the SNR value for each subcarrier (ϱ_s), as opposed to a single average value as in the general SNR metric. The subcarrier-specific SNR is then aggregated into a global metric, *effectiveSNR* (eSNR), which better characterizes channel performance. We next provide an introduction to CSI.

B. Channel State Information

Wireless signals experience transformations such as amplitude and phase changes while traveling over the air from the transmitter to the receiver. For example, a simple model is

$$y[t] = h \cdot x[t] + z[t], \tag{1}$$

where t is a time index, y is the received signal, x is the transmitted signal, h is the channel gain, or more often a complex value representing both channel gain and phase component, and z is additive noise. More complex models incorporate multipath fading, time-varying channels, multiple antennas, etc. Coherent receivers require knowledge of CSI (h in the simple model (1) above) for successful demodulation. CSI can also be used for data rate selection, antenna selection, power control and allocation across transmit antennas, etc.

One method of obtaining CSI is to use pilot sequences within the data packet. These sequences are predetermined sequences (i.e., they do not carry information) that are sent within the data packet to help the receiver estimate CSI. For example, in the channel model (1), setting $x = 1$ in the first k symbols of the data packet allows the receiver to compute

$$\hat{h} = \frac{\alpha}{k} \sum_{t=1}^{k} y[t] = \alpha \cdot h + \frac{\alpha}{k} \sum_{t=1}^{k} z[t] \tag{2}$$

where the constant α is chosen appropriately depending on the SNR.

The 802.11n protocol allows the use of MIMO to obtain improvements in data rate and reliability. In addition, 802.11n uses OFDM modulation to convert a wideband channel into multiple narrowband channels to avoid inter-symbol interference (ISI). The simple model (1) can be extended for a MIMO OFDM system as follows:

$$\mathbf{y}[w,t] = H[w]\mathbf{x}[w,t] + \mathbf{z}[w,t] \tag{3}$$

where for n transmit and m receive antennas, $\mathbf{x}$ is an n-dimensional vector, $\mathbf{y}$ and $\mathbf{z}$ are m-dimensional vectors, H is an $m \times n$ matrix, and w is an index specifying the OFDM frequency channel. In MIMO OFDM systems, the CSI H is an $m \times n \times W$ data structure, where W is the number of OFDM channels used in the system ($W = 56$ in 802.11n for 20 MHz bandwidth, and $W = 114$ in 802.11n for 40 MHz bandwidth with channel bonding). Note that in (3) the column index of $H[w]$ indicates the transmit antenna index, while the row index of $H[w]$ corresponds to the receive antenna index.

C. CSI Estimation in 802.11n

Many implementations of 802.11n require successful decoding of a data packet to obtain CSI. In addition, it is required to send a packet using n transmit antennas over a bandwidth W, and receive it over m receive antennas to obtain the complete $m \times n \times W$ CSI data structure. In the following, we denote any type of communication scheme that involves n transmit antennas, m receive antennas, and spans a bandwidth W as an $m \times n \times W$ configuration.

In current CSI estimation approaches, obtaining CSI for all possible configurations of a 3×3 system requires seven samples: 1-stream Modulation and Coding Schemes (MCS) require three probes, one per each TX antenna. Similarly, 2-stream MCSs require three probes to collect CSI for each combination of two antennas. Finally, 3-stream MCSs require a single probe using a transmission from all three transmit antennas. The number of required samples increases dramatically when the system supports 4×4 communication or larger channel widths. Moreover, common hardware only provides CSI reports for unicast packets, thus limiting the possibility of opportunistically collecting CSI matrices by eavesdropping; a node must be connected to an access point to actively send or receive probing packets.

In the rest of this paper, we discuss the problem of estimating $p \times q \times R$ CSI data structures using packets encoded with $m_i \times n_i \times W_i$ schemes, where $p \geq m_i$, $q \geq n_i$, $R \geq W_i$, and $(p, q, R) \neq (m_i, n_i, W_i)$, where i is the packet index. We then show how CSI data structures obtained from multiple packet transmissions can be used to to estimate *larger* CSI data structures. We describe this problem in the context of an

802.11n system. However, similar ideas can be applied to CSI estimation in other MIMO OFDM systems (e.g. WiMAX).

III. CSI-SF

CSI-SF reduces the overhead of channel probing by aggregating the CSIs obtained from multiple packets from a smaller channel to derive the CSI corresponding to a larger channel. For example, CSI-SF enables the determination of a $2 \times 2 \times 56$ CSI matrix by combining the CSI information derived from two packets transmitted using a $2 \times 1 \times 56$ configuration, as long as different transmit antennas are used to send the two packets. Combining the CSI from multiple packets can be used to:

- estimate a larger multi-antenna $m \times q \times W$ CSI matrix using packets sent/received with a smaller multi-antenna $m \times n \times W$ configuration (i.e., $q > n$);
- estimate a larger bandwidth $m \times n \times R$ CSI matrix using packets sent/received with an smaller bandwidth $m \times n \times W$ configuration (i.e., $R > W$);
- estimate a CSI matrix combining the above two cases (i.e. enlarge the number of antennas and bandwidth in the combined CSI).

A. Enlarging the Number of Antennas or Bandwidth in the CSI Matrix

The key benefit of CSI-SF is in combining CSI from multiple packets to create a CSI matrix corresponding to more transmit antennas than those used in the given packets. To capture the space of this combination, let $\mathcal{N}_i$ be the set of antennas used in packet i, of size $|\mathcal{N}_i|$, and let $\mathcal{N}$ be the set of transmit antennas in the combined CSI matrix. We assume that $|\mathcal{N}| > |\mathcal{N}_i|$ for all $i \in \mathcal{I}$, where $\mathcal{I}$ is the set of packets used to combine the CSI. We require $\mathcal{N} \subset \cup_i \mathcal{N}_i$ so that we have CSI for all transmit antennas in $\mathcal{N}$.

Combining CSI from a smaller set of transmit antennas to infer CSI matrix for a larger set of antennas requires that the transmitter changes the set of transmit antennas used in each packet. In addition, the set $\mathcal{N}_i$ of transmit antennas used in packet i needs to be identified within the packet. This can be done, for example, by adding metadata about $\mathcal{N}_i$ to the header or payload of the packet. Similarly, CSI combining used to enlarge the number of frequency subchannels in the CSI matrix (e.g., to go from 20 MHz to 40 MHz bandwidth) needs different packets transmitted in different channels (e.g., channels 36 and 40 of the 5 GHz band) so that CSI derived from those packets can be combined to estimate the CSI matrix of the bonded channel 36+40.

B. Power Scaling

The CSI estimates produced by the receivers are dependent on the transmission power used for the packet. However, if transmission power is constant, CSI combining does not depend on transmission power. Essentially, if the channel gains remain constant during the transmission of the two packets and $P_2 = \gamma P_1$, where P_i is the transmission power of packet i, $i = \{1, 2\}$ and γ is a scale factor, then $\text{CSI}_2 = \sqrt{\gamma}\text{CSI}_1$, where CSI_i is the CSI estimate produced for packet i.

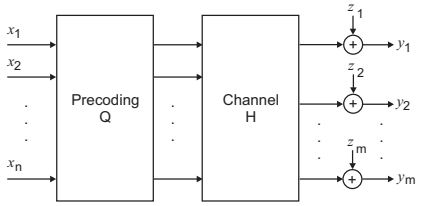

Fig. 1. MIMO channel with precoding matrix Q. The dependency on time or frequency is omitted.

Due to regulations and practical limitations, transmitted signals have a total power constraint. When the transmission spans multiple transmit antennas, assuming that the signals in the different antennas and OFDM sub-channels are statistically independent, the total transmitted power is given by $P = \sum_{w=1}^{W} \sum_{i=1}^{n} P_i[w]$, where $P_i[w]$ is the power in the signal transmitted in antenna i, $i = 1, \ldots, n$ and frequency sub-channel w, $w = 1, \ldots, W$. In order to satisfy the total power constraint, $P_i[w]$ may vary for different configurations with different bandwidths or number of transmit antennas, even when the power settings specified by the driver is the same.

These power considerations have important implications for CSI combining. Since the transmission powers may not be known at the receiver (see Model (3)), the CSI estimate for entry (i, j) in sub-channel w of the channel matrix H may be an estimate of $H_{i,j}[w]\sqrt{P_j[w]}$. Since $P_j[w]$ may vary for communication schemes involving different numbers of transmit antennas and different transmission bandwidths, CSI estimates must be appropriately scaled during CSI combining. If the total power setting is not changed between packets, this scaling is based only on the number of streams, and no information about the power settings at the transmitter is required.

C. Precoding

Spatial multiplexing is achieved by sending different data streams in the different entries of $\mathbf{x}$ (see Model (3)). The 802.11n standard allows the use of a precoding matrix Q to map $\mathbf{x}$ into the channel. Typically, Q is a unitary matrix (i.e. $Q \cdot Q^\dagger = Q^\dagger \cdot Q = I$, where † denotes conjugate transpose and I is the identity matrix). Equation (3) represents the so-called *direct mapping* mode, in which $Q = I$ and each data stream is sent in a different transmit antenna. More generally, the received signal vector can be written as (see Fig. 1)

$$\mathbf{y}[w, t] = H[w]Q\mathbf{x}[w, t] + \mathbf{z}[w, t]. \quad (4)$$

Typically, the precoding matrix Q does not need to be known at the receiver, and the channel estimation algorithm provides an estimate of $H[w]Q$. The CSI-SF combining technique requires the receiver to know Q and post-multiply the channel estimates $\hat{H}[w]$ by $Q^\dagger$ or Q^{-1} if Q is not unitary (i.e., $\hat{H}' = \hat{H} \cdot Q^\dagger$). However, Q varies based on the chipset used, and may also be changed adaptively. In the rest of this section, we assume that Q is known. In Section IV, we investigate the loss in performance of implementing a Q-agnostic estimator.

To understand the combining process, consider the following example illustrating how to combine CSI from two packets

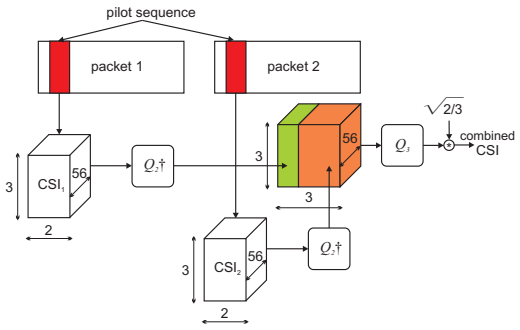

Fig. 2. Schematic representations of the operations used to combine CSI from multiple packets.

sent/received with an $3 \times 2 \times 56$ configuration and precoding matrix Q_2 to form a CSI estimate for a $3 \times 3 \times 56$ configuration (see Fig. 2). We assume that $\mathcal{N}_1 = \{1, 2\}$, $\mathcal{N}_2 = \{2, 3\}$ and $\mathcal{N}_\ni = \{1, 2, 3\}$. Similar operations are performed for the remaining 55 sub-channels. After successful reception of packet i, $i \in \{1, 2\}$, the receiver generates a CSI estimate for sub-channel w, $\hat{H}_i[w]$, which may be dependent on the transmission power in each antenna and frequency sub-channel. Next, the receiver post-multiplies $\hat{H}_i[w]$ by $Q_2^\dagger$ obtaining $\hat{H}'_i[w] = \hat{H}_i[w] \cdot Q_2^\dagger = [\hat{\mathbf{h}}_{1,i}[w], \hat{\mathbf{h}}_{2,i}[w]]$, where $\hat{\mathbf{h}}_{i,j}[w] \in \mathbb{C}^2$, $i, j \in 1, 2$. The combined CSI for sub-channel w, after power scaling, is given by

$$\hat{H}_3[w] = \sqrt{\frac{2}{3}} \cdot [\hat{\mathbf{h}}_{1,1}[w], \hat{\mathbf{h}}_{1,2}[w], \hat{\mathbf{h}}_{2,2}[w]] \cdot Q_3.$$

Note that $\hat{\mathbf{h}}_{2,1}[w]$ and $\hat{\mathbf{h}}_{1,2}[w]$ contain CSI that can be used to generate $\hat{H}_3[w]$. CSI-SF only used $\hat{\mathbf{h}}_{1,2}[w]$ in the combined CSI estimate because wireless channels often experience variations over time and the most recent CSI is often the most suitable to make future estimates. However, more general combining functions can be used to balance the effects of channel variations and channel estimation errors due to, for example, noise. One such example is

$$\hat{H}_3[w] = \sqrt{\frac{2}{3}} \cdot [\hat{\mathbf{h}}_{1,1}[w], (\beta \hat{\mathbf{h}}_{1,2}[w] + (1-\beta)\hat{\mathbf{h}}_{2,1}[w]), \hat{\mathbf{h}}_{2,2}[w]] \cdot Q_3,$$

where $\beta \in [0, 1]$is some constant chosen appropriately.

D. Transmission Power Compensation

In most WLAN deployments, dynamic transmission power is used in combination with rate control to reduce energy consumption. Commodity hardware allows the user to choose a transmission power level. If the transmitted power closely follows the level chosen by the user, a scale factor can be applied to the CSI of a packet transmitted at a specific power level to estimate the CSI of a different power level. For example, if a receiver receives a packet sent at 7 dBm and is interested in the estimated CSI for a transmission with the same antenna configuration at 5 dBm, it is enough to subtract 2 dB from the magnitude of the original CSI to obtain the new one.

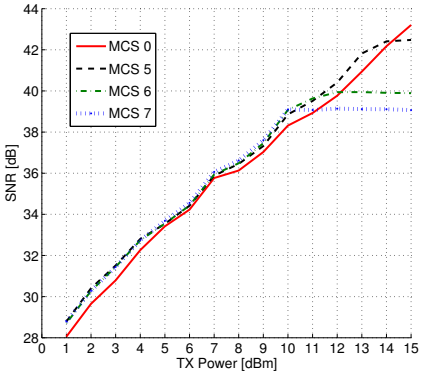

Fig. 3. SNR for different tx power levels for four 1-stream MCSs.

However, practical limitations influence the power control capabilities of real transceivers. Power amplifiers are not perfectly linear, producing increasing distortion as they are driven closer to their maximum rated power. The distortion introduced by the transmitter amplifiers has a bigger impact on MCSs with larger coding rates and higher order modulations. As a result, many transceivers limit the output power used for high rate MCSs through various *power caps*. Figure 3 shows these power caps for QAM-64 transmissions with different coding rates. The same behavior is present for 2- and 3-stream MCSs, but the linear region extends to higher power settings. This is most likely a result of the fact that for multiple stream packets the power is split among the multiple streams, reducing the power that each amplifier is required to output.

An accurate power profiling can prevent two erroneous outcomes in the CSI estimation procedure. First, when using the CSI derived from a packet with a specific MCS to estimate the CSI of a different MCS, not being aware of the power caps might introduce estimation errors. This happens not only when combining CSI to produce estimates for a different number of streams, but also when using the CSI from a given MCS to estimate the CSI for some other MCS with the same number of streams. Additionally, this information must be considered when estimating the effect of power adaptation. For example scaling the nominal transmission power from 10 dBm to 15 dBm has no effect on the actual transmitted power (and power consumption) in MCS7.

To correct power scaling requires two pieces of information:

- The power profile for the specific hardware installed in the transmitter. This information can be hard coded in the receiver or sent on demand by the transmitter.
- The power level at which each packet is sent. This information can be specified explicitly by the transmitter with a d control packet or attaching it to data packets, or inferred from the packet type (e.g., beacons are generally transmitted at the lowest data rate and the highest power level).

The 802.11n standard provides an *optional* feature called staggered sounding by which the training sequence in the packet header is transmitted over more streams than those used in the payload of the packet. This feature would enable

us to learn a larger CSI structure without risking a decoding error in the payload of the packet. While this feature would solve the same problem that we are addressing, it presents a number of drawbacks and practical limitations. First, being an optional feature, it may not be supported across different chipset vendors. In addition, it does not allow estimating CSI structures for larger bandwidth than that used for the given packet. Finally, it is not supported during beacon transmissions, hence it cannot be used in applications such as AP selection during association. When staggered sounding is supported, it can be used jointly with CSI-SF to further reduce the number of samples required to obtain complete knowledge of the MIMO channel.

We next evaluate the performance of CSI-SF, and also investigate the impact of approximations that may be necessary due to the lack of knowledge of the hardware-specific Q matrix and power profile.

IV. EVALUATION

We evaluated the performance of CSI-SF using CSI information collected on our 802.11n testbed. We deployed five nodes, equipped with an Intel 5300 chipset that supports up to 3×3 MIMO configurations. A modified chipset firmware and kernel [18] were used to obtain the CSI matrices of successfully received 802.11n data frames and transfer the matrices to userspace for further analysis. We deployed the nodes in a cubicle office environment. At different times, each node took turns to serve as an AP on a free channel in the 5 GHz spectrum and sent packets at various MCS rates and transmission powers, while the other nodes, associated to the AP, collected the CSI for received packets. We performed the tests multiple times with different placements of nodes thus collected data from 30 different links in total. For each power level and transmission antenna combination, we changed the MCS after each packet, and collected CSI for 1,000 packets at each MCS, with an average inter packet arrival time of 1 ms, which is the time necessary for the driver to change the hardware settings. We performed the same experiments in the 2.4 GHz band, and obtained similar results that we omit for space constraints.

The Intel hardware only reports CSI for a subset of the OFDM subcarriers, as defined by the *grouping* option in the 802.11n standard. More specifically, it reports CSI for 30 subcarriers in either the 20 MHz or the 40 MHz bonded channel (grouping 2 and 4, respectively).

A. Single Stream to Multi Stream Combining

CSI-SF's main goal is to predict the CSI of channel configurations that have not been sampled, by using a proper combination of packets sent with a smaller number of spatial streams. We first compare the CSI obtained from combining the CSI of two 1-stream packets sent over two different transmission antennas against the actual CSI of the 2-stream configuration, sampled immediately after the two 1-stream samples were collected. For a 1-stream packet, the Intel 5300's CSI structure is a $1 \times 3 \times 30$ matrix, and for a 2-stream packet it is a $2 \times 3 \times 30$ matrix. In Figure 4, we plot the magnitude of each element of the CSI matrices of the two 1-stream packets (top) and

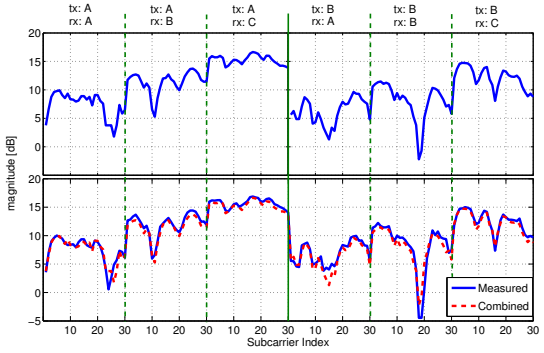

Fig. 4. Magnitude of each CSI element for two 1-stream packets (top) and their 2-stream combination, compared with an actual 2-stream packet (bottom).

compare the resulting combined CSI with the actual 2-stream CSI (bottom). The combined and actual CSI are only slightly different probably due to small channel variations between the time at which the three packets were sampled. However, the difference is small, and when CSI is used to compute aggregate metrics such as eSNR, it becomes negligible. More details are provided in the following subsections.

The accuracy of a combined estimate depends on the freshness of samples used in the combining algorithm. The office environment in which we collected the samples does not show significant channel variations over time, and therefore an estimate from aged packets could be used. In a more dynamic environment, the accuracy of the CSI-SF estimates would degrade, but so would the accuracy of any probing mechanism.

B. e^2*SNR:* estimated *effectiveSNR*

While a complete characterization of a given channel by looking at every element of its CSI matrix might be useful at times, in most applications (e.g., bitrate adaptation) an aggregate metric obtained from the CSI is sufficient. Hence we use the *effective SNR* (eSNR) value, as described in [15], to evaluate the accuracy of CSI-SF. eSNR first computes the SNR and bit-error rate (BER) of each OFDM subcarrier. From the subcarrier-specific information, a channel-wide BER is computed and translated into eSNR. The accuracy of eSNR in terms of describing the quality of OFDM MIMO channel compared with the per-packet SNR metric that 802.11 drivers usually provide in the form of Received (or Relative) Signal Strength Indicator (RSSI) is shown in [15]. In the rest of this section, we use the term, SNR, to indicate the per-packet SNR directly given by drivers.

We evaluate the accuracy of CSI-SF by comparing the eSNR obtained from the real CSI information against eSNR obtained using CSI-SF, which we call *estimated effective SNR* (e^2SNR). Figures 5 and 6 show the relation between each metric (SNR, eSNR and e^2SNR) and the maximum supported rate on 2×3 links we tested on various environments and configurations. We say that a bitrate is "supported" by a given link when the packet error rate at that bitrate is measured to be smaller than

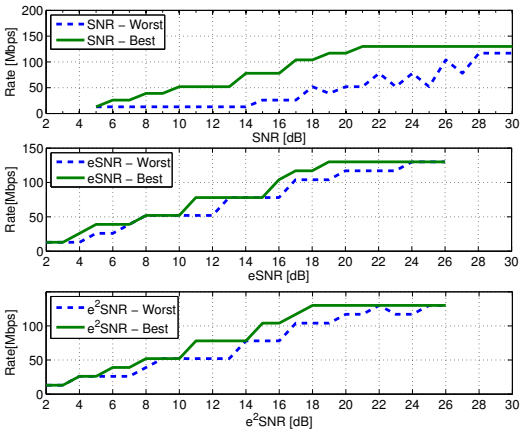

Fig. 5. Link rates (Mbps, y-axis) for the best and the worst links as a function of various metrics (SNR, eSNRand e^{2}SNR) for 2-stream MCSs using a *20 MHz* channel.

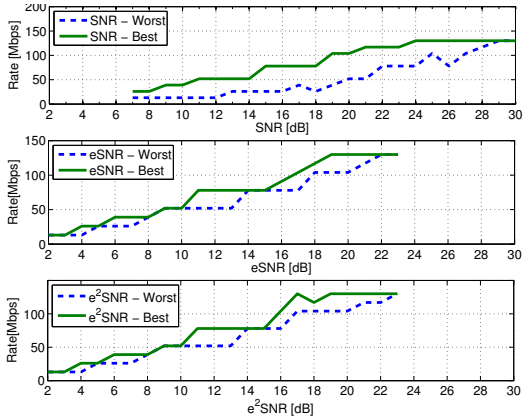

Fig. 6. Link rates (Mbps, y-axis) for the best and the worst links as a function of various metrics (SNR, eSNRand e^{2}SNR) for 2-stream MCSs using a *40 MHz* channel.

10%. We define "link rate" the maximum supported bitrate for a link. For rate adaptation algorithms and similar applications, it is imperative that the link quality metric shows a predictable behavior. However, for each metric, it is possible that links with the same metric value support different link rates. For each value of SNR, eSNR and e^{2}SNR we find the link with the highest and the lowest link rate and denote them as the *best* and the *worst* links, respectively. For each metric we plot the link rate for the best and the worst link. A good metric should exhibit two properties:

- a small gap between the best and the worst links (ideally the two lines should overlap) to enable an accurate prediction of the link rate;
- a monotonic relation between the metric value and the link rate, so that we can always consider a higher metric value as a better link quality indicator.

In both Figures 5 and 6, each from 20 MHz and 40 MHz channel widths respectively, the use of packet SNR (the top graphs) results in significant gaps between the bitrates supported by the best and the worst links with the same SNR value. A rate selection algorithm based on SNR could choose to be conservative and select a low bitrate, and then increase the rate until the link rate is reached, or be optimistic and start from the bitrate supported by the best link with the same SNR value and then fallback to a lower rate if the selected one is not supported. In both cases the algorithm takes time to converge to the optimal rate. The bottom part of the figures show the results of using eSNR and e^{2}SNR metrics. For the most part, the best and the worst link overlap or show a small gap limited to one MCS difference, which suggests that an accurate estimate of the supported bitrate for a link is possible. Additionally, *e^{2}SNR from combined CSI exhibits a promising bitrate predictability, which is comparable to that of eSNR of actual CSI.*

C. Effect of Unknown Q Matrix

For the hardware we used in the experiments, we had complete knowledge of the spatial mapping matrix (Q) for the 2-stream settings. In Section III, we described why knowing Q is necessary for computing the correct CSI for combining. However, hardware vendors might not always disclose this information and even when it is known at the transmitter, informing the receiver would require additional overhead. We investigated the effect of using inaccurate Q matrix through MATLAB simulations. Our goal is to evaluate the effect of applying an inaccurate Q to the received CSI on the final metric (e^{2}SNR). We randomly generated $10,000$ H matrices, with 30 subcarriers each. The elements of the matrices are generated with a circularly symmetric complex Gaussian distribution with variance 1, $\mathcal{CN}(0,1)$. For each of these channels we computed the CSI applying a TX power ranging from 10 dB to 40 dB (this value is normalized with the noise level) and using the identity matrix as a spatial mapping matrix (i.e., each data stream is independently transmitted by each antenna). We also generated 500 random Q matrices (unitary) and for each of the CSI matrices we computed the eSNR using all the different Q matrices. *The standard deviation of the eSNR values obtained using the* 500 *different values of Q, averaged over* $10,000$ H *is smaller than* 1 *dB.* Considering that 1 dB is the granularity that all the metrics assume, and a difference of 1 dB means at most an error of one MCS, the metric without knowledge of Q can still be used, although the precision of the fine granularity estimation in Figure 4 is lost.

We also tested the effect of using a wrong Q matrix also with our real testbed, using four different values of Q (i.e., the correct one, the identity matrix, and two randomly generated matrices). The results, which we omit for space constraints, showed none or very small differences compared with those in Figures 5 and 6.

In contrast to 2-stream cases, the exact Q matrix for the 3-stream MCSs is not known to us and thus we use the identity matrix instead. The results using the identity matrix for 3-stream is shown in Figure 7. The same remarks we made for the 2-stream experiments can be applied for this experiment as well, with the addition that in this case not only the gap between the worst and the best link for the packet SNR metric is very

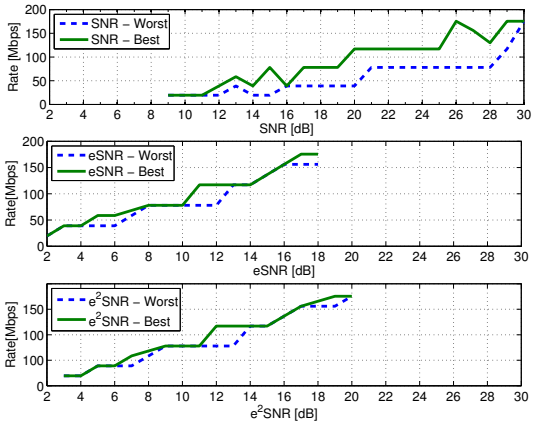

Fig. 7. Link rates (Mbps, y-axis) for the best and the worst links as a function of various metrics (SNR, eSNRand e^2SNR) for 3-stream MCSs using a *20 MHz* channel.

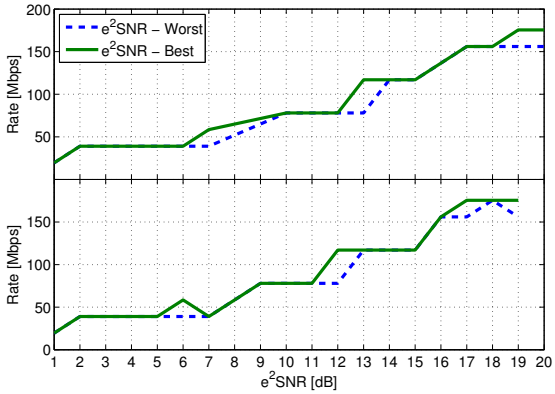

Fig. 8. Relation between e^2SNR link rate for the best and the worst links, when applying power compensation (top) or ignoring it (bottom).

large, but in some cases (e.g., between 12 dB and 16 dB) the relation between SNR and the supported rate is non-monotonic. The results for eSNR and e^2SNR are once again very similar. The supported rate is monotonically increasing and the gap between the best and the worst link is never larger than 2 MCS steps (in fact, a two MCS gap is shown only for values of eSNR and $e^2\text{SNR} \geq 17$ dB). There is no significant difference in the performance of the two metrics. These results show that CSI-SF achieves high accuracy while reducing the probing overhead.

D. Channel Width Expansion

CSI-SF not only can be used for estimating a MIMO configuration with a larger number of antennas, but also for a channel that is bonding two or more narrower channel which have been sampled independently. Bonding of two adjacent channel is used in 802.11n to increase the bandwidth, and the new 802.11ac standard allows bonding of non-adjacent channels up to a bandwidth of 160MHz. We tested the accuracy of CSI-SF on bonded channels by comparing the e^2SNR obtained from combining two 20MHz link sent on different channels, and the actual eSNR of packets sent on the bonded channel, on several different links. *The maximum value for the standard deviation is lower than 2 dB*. The distance between the synthetic e^2SNR and the real eSNR can be explained with the large time between the arrival of packets on the different channels in our experiments, due to hardware configuration constraints.

Note that the reported CSI has only a subset of the OFDM frequencies. For the 40MHz channel, three out of four subcarrier are not reported from the Intel hardware. This lack of information causes the eSNR itself to be imprecise. A more accurate evaluation using hardware capable of reporting CSI for entire subcarriers is our future work.

E. Power Compensation

In Section III, we described the non-linear relation between the power settings and the transmitted power at different MCSs. When the hardware-specific power profile is known, the receiver can compensate it when applying CSI-SF. For example, when combining two 1-stream packets sent at MCS 7 with a power setting of 15 dBm, we must consider that the real transmitted power is 11 dBm (Figure 3). If the combined CSI is used to compute the e^2SNR of a 2-stream MCS with no power cap, for example MCS 8, we must compensate for a 4 dB offset or the quality of the combined CSI will be underestimated.

However, as the power profile is a property of the hardware, there might be situations in which the receiver does not know what is the proper compensation to apply. In Figure 8 we compare the e^2SNR performance with the proper power compensation (top) against the same metric, computed ignoring the power profile (bottom). We combined only packets sent with MCS6, using transmission power settings between 10 dBm and 15 dBm, to see the difference more clearly. The most visible effect of the lack of power compensation is the compression of the values in the x-axis, due to the fact that the combining algorithm tends to overestimate the power at which the original packets are sent, which in reality is lower than the level specified by the driver.

Our power compensation algorithm adds the offset to the CSI before using it in the combining algorithm, to correct this behavior. However, we observe that even when power compensation is not applied, although e^2SNR and eSNR curves differ, e^2SNR still shows the two desirable characteristics of a good channel quality metric. However, the x-axis shift, caused by the lack of power compensation, requires training to identify the shifted metric-to-MCS mapping. Fortunately, even in this case, the relation between e^2SNR and the supported rate depends on the hardware but not on individual link. Thus, in case of downlink MCS adaptation, a receiver must train only once when it associates with an AP based on a specific hardware, and use that information for any other link as long as the AP uses the same hardware. Once the training is performed and the mapping is stored, no additional overhead is required.

V. CSI-SF Application

CSI-SF can be used to obtain a complete characterization of the channel, without incurring the same overhead of traditional probing. The estimated CSI can be used to improve network performance in many ways. In this section, we describe possible uses of CSI-SF in three common WLAN protocol applications.

1-stream TX antenna	Best MCS (bitrate)	2-stream TX antenna	Best MCS (bitrate)	3-stream TX antenna	Best MCS (bitrate)
a	7 (65 Mbps)	ab	14 (117 Mbps)	abc	18 (58.5 Mbps)
b	7 (65 Mbps)	bc	13 (104 Mbps)		
c	6 (58.5 Mbps)	ac	12 (78 Mbps)		

(a) Best MCS for different TX antenna combinations of a given link.

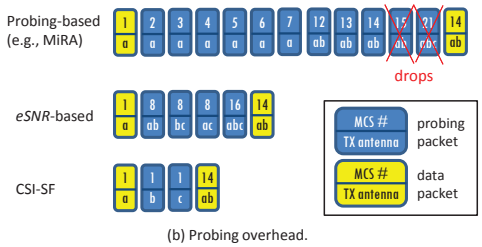

(b) Probing overhead.

Fig. 9. Probing overhead comparison on an example 3×3 link.

A. Optimal MCS and Antenna Selection

Bitrate adaptation is necessary to maximize the achievable throughput in a dynamic wireless link. In legacy SISO channels, the space to search for the best bitrate is limited to the number of modulation and coding schemes, which is eight in the case of 802.11a/g systems. The use of multiple antennas and MIMO channel coding adds one more dimension. With the conventional probing-based approach that relies on packet error statistics for every possible bitrate, the probing overhead (or the search space size) is asymptotically $O(n^2ck)$, where n is the number of possible streams (usually equal to the number of TX antennas), c is the number of modulation & coding schemes for each stream (8 in 802.11 systems) and k is the number of required probings for each rate to obtain enough statistics. The n^2 overhead stems from the number of possible TX antenna combinations. If the optimal antenna selection is not supported, the asymptotic overhead becomes $O(nck)$ but the chance of finding the best bitrate decreases.

The use of CSI for MCS adaptation, as shown in [15], [17] by using the eSNR metric, greatly reduces probing overhead and also convergence time because a single CSI matrix can directly indicate the best MCS supported by the channel from the MCSs using the same number of MIMO streams, thus removing the c and k factors. Hence, the overhead of eSNRbased adaptation schemes is $O(n^2)$. Furthermore, CSI-SF does not need to probe all possible TX antenna combinations to compute e^{2}SNR for all MCSs. It only needs n 1-stream CSI samples, with each sample from the n TX antennas.

Figure 9 illustrates the probing overhead of three different approaches: a probing-based MIMO link adaptation scheme (e.g., MiRA [19]), an eSNR-based scheme and CSI-SF. Since [15] does not describe an adaptation mechanism for changing MCS over different numbers of streams and antennas over a time-varying channel, we simulate the best possible behavior of an eSNR-based adaption scheme. Figure 9(a) shows the best MCSs for all TX antenna combinations that we observed from one example 3×3 link of our testbed. The 2-stream MCS 14 on two TX antennas 'ab' (out of three antennas 'a', 'b' and 'c') exhibited the best throughput performance on that link. Next consider a change in the environment where channel quality has improved from the case when MCS 1 was the best MCS. Figure 9(b) shows that the probing-based scheme probes all 1-stream MCSs above the current rate and all the 2-stream MCSs that provide higher rates than MCS 7.[1] MCS 15 fails because this channel can only support up to MCS 14. MCS 21 is also probed because this is the lowest 3-stream MCS that could provide a higher rate than MCS 14 but this MCS also fails since MCS 18 is the highest 3-stream MCS supported by this link. As a result, a total of 11 probes are required and the actual probing overhead would be much larger for a statistically meaningful outcome. As mentioned in [19], 802.11n AMPDU aggregation can be used to mitigate the probing message overhead but the overhead is still much larger than the CSI-based schemes. Unlike MiRA, where the payload size impacts the packet error rates, the probing packets to obtain CSI matrices do not need any data payload. 802.11n's optional null data packet sounding can be used to obtain CSI samples with minimal message overhead.

Figure 9(b) clearly illustrates that the eSNR-based scheme and CSI-SF incur much smaller probing overhead and quickly find the best MCS. We hence expect them to perform even better in mobile environments. In this example, the eSNR-based scheme must probe all three TX antenna combinations of 2-streams to discover MCS 14 transmitted over 'ab' is the best one. The 3-stream MCS 16 is also probed to check if there is any 3-stream MCS that provides a better bitrate than MCS 14; thus four probings are used in total. In contrast, CSI-SF uses only two probings and combines their CSI matrices with the one from the 1-stream data packet and decides the best MCS and the antenna combination. If we expand this example to 4×4 MIMO, the probing overhead reduction of CSI-SF from eSNR is from 11 to 3.

B. Channel Bonding in 802.11ac

The new IEEE 802.11ac standard, currently being defined, is exploring the option of using up to eight 20 MHz channels for the bonding feature. Similar to 802.11n, the proposed scheme defines one of the 20 MHz channel as the primary channel, while the others are secondary channels, and can be dynamically used if necessary. A station can choose to operate (i) using only the primary channel, (ii) leveraging the whole 160 MHz bandwidth or (iii) selecting one or three secondary channels to be used in conjunction with the primary channel. Note that the secondary channels are not required to be adjacent. Based on the bonding scheme currently discussed in the standard group [20], [21], there are a total of 44 possible channel combinations that a probing-based mechanism should examine. Using the channel expansion mechanism in CSI-SF, only eight samples are necessary, one per 20 MHz channel, to compute a complete characterization of all the possible bonding combinations.

[1]For simple illustration, we assume this probing-based scheme does not select antennas optimally but uses antenna combinations of 'a', 'ab', and 'abc', which favor this exemplary scheme since the best MCS is from 'ab'.

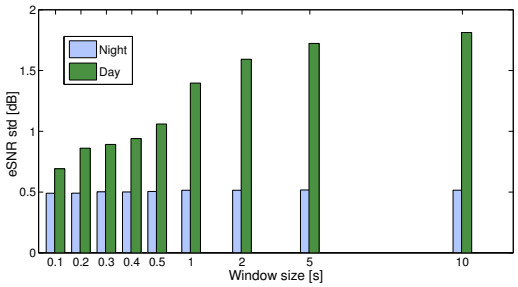

Fig. 10. Average standard deviation of eSNR value for different sizes of a sliding window. We compare two different links measured at different times of the day.

C. AP Association

Another case where CSI-SF is useful is when a client must decide which AP to associate with. Our experiments confirmed that the AP that has the strongest SNR might not be the one with the highest supported rate. CSI and eSNR for the MIMO configurations would be a better metric, but 2- and 3-stream packets can only be received after associating with an AP. However, three 1-stream beacons, sent from each AP on its three antennas, would suffice for our algorithm to compute the e^2SNR of all MIMO configurations for each AP. To support this application, an AP must simply switch the antenna from which the beacons are sent, an easy variation on traditional AP behavior with no effect on clients that do not implement CSI-SF.

Of course this measurement is only valid as long as the channel quality is stable, but this limitation applies to all AP selection algorithms. For our experimental settings, we studied the average standard deviation of the eSNR of packets received in temporal windows of various sizes for the links that we used in our experiments. We compare the results of two links in Fig. 10. The traces were collected in the same office environment, one of them during daytime, with no node mobility but people freely moving in the space surrounding the two nodes, and the other during the night when the office was empty. The night environment is quite steady, although interestingly it shows a certain amount of variation, independent from the length of the window. However, in both cases, the average standard deviation is below 1dB for up to 500ms, and does not exceed 2dB even for the largest window tested. This is an indication that even in a busy office environment, when nodes are not mobile, the link rate estimated before the association is likely to remain constant for a long period.

VI. Conclusion

This paper presents CSI-SF, a method for estimating CSI using a small number of frame transmissions and extrapolating data to settings that have not been sampled. We implemented and evaluated CSI-SF on our 802.11n network testbed and also discussed the practical challenges of CSI-SF. In our experiments in various network scenarios, CSI-SF showed high efficiency and effectiveness by achieving high accuracy in CSI estimation with reduced sampling overhead. CSI-SF can be utilized not only for estimating CSI for larger number of streams, but also for wider channels and different transmission power levels. We also showed that CSI-SF provides accurate estimates even without knowledge of hardware specific characteristics such as non-linear response to the power settings and unknown spatial mapping matrix. We believe the algorithm designers for rate adaptation, beamforming, association control can take advantage of CSI-SF to improve their performance. We also argue that CSI-SF will be even more beneficial in future networks with more antenna configurations and wider bonded channels.

References

[1] A. Balasubramanian, R. Mahajan, and A. Venkataramani, "Augmenting mobile 3G using WiFi," in *Proceedings of ACM MobiSys*, 2010.

[2] "IEEE 802.11n-2009 Amendment 5: Enhancements for Higher Throughput," IEEE-SA. 29 October 2009.

[3] "IEEE 802.11ac: Very High Throughput $<$ 6 GHz," IEEE Standards.

[4] A. J. Paulraj, D. A. Gore, R. U. Nabar, and H. Bolcskei, "An overview of MIMO communications - a key to gigabit wireless," *Proceedings of IEEE*, vol. 92, no. 5, 2004.

[5] A. Goldsmith, S. A. Jafar, N. Jindal, and S. Vishwanath, "Capacity limits of MIMO channels," *IEEE Journal on Selected Areas in Communications*, vol. 25, no. 5, 2003.

[6] A. Kamerman and L. Monteban, "WaveLAN-II : A High-Performance Wireless LAN for the Unlicensed Band," *Bell Labs Technical Journal*, pp. 118–133, July 1997.

[7] M. Lacage, M. H. Manshaei, and T. Turletti, "IEEE 802.11 rate adaptation: a practical approach," *Proc. of MSWiM*, p. 126, 2004.

[8] T. Joshi, D. Ahuja, D. Singh, and D. Agrawal, "SARA: Stochastic Automata Rate Adaptation for IEEE 802.11 Networks," *IEEE Transactions on Parallel and Distributed Systems*, vol. 19, no. 11, pp. 1579–1590, Nov. 2008.

[9] J. Choi, J. Na, Y.-s. Lim, K. Park, and C.-k. Kim, "Collision-aware design of rate adaptation for multi-rate 802.11 WLANs," *IEEE Journal on Selected Areas in Communications*, vol. 26, no. 8, pp. 1366–1375, Oct. 2008.

[10] J. Kim, S. Kim, S. Choi, and D. Qiao, "CARA: Collision-Aware Rate Adaptation for IEEE 802.11 WLANs," in *Proc. of IEEE INFOCOM*. IEEE, Apr. 2006, pp. 1–11.

[11] S. H. Y. Wong, H. Yang, S. Lu, and V. Bharghavan, "Robust rate adaptation for 802.11 wireless networks," *Proc of ACM MOBICOM*, p. 146, 2006.

[12] G. Holland, N. Vaidya, and P. Bahl, "A rate-adaptive MAC protocol for multi-hop wireless networks," *Proc. of ACM MOBICOM*, 2001.

[13] K. LaCurts and H. Balakrishnan, "Measurement and analysis of real-world 802.11 mesh networks," in *Proc. of ACM IMC*, Nov. 2010.

[14] A. Willig, M. Kubisch, C. Hoene, and A. Wolisz, "Measurements of a wireless link in an industrial environment using an IEEE 802.11-compliant physical layer," *IEEE Transactions on Industrial Electronics*, vol. 49, no. 6, pp. 1265–1282, Dec. 2002.

[15] D. Halperin, W. Hu, A. Sheth, and D. Wetherall, "Predictable 802.11 packet delivery from wireless channel measurements," in *Proc. of ACM SIGCOMM*, 2010.

[16] S. Nanda and K. Rege, "Frame error rates for convolutional codes on fading channels and the concept of effective eb/n0," *IEEE Transactions on Vehicular Technology*, vol. 47, no. 4, pp. 1245–1250, 1998.

[17] T. Tao and A. Czylwik, "Performance analysis of Link Adaptation in LTE systems," in *International ITG Workshop on Smart Antennas (WSA)*. IEEE, 2011, pp. 1–5.

[18] D. Halperin et al., "802.11n CSI Tool based on iwlwifi and Linux-2.6," https://github.com/dhalperi/linux-80211n-csitool-supplementary.

[19] I. Pefkianakis, Y. Hu, S. H. Wong, H. Yang, and S. Lu, "MIMO Rate Adaptation in 802.11n Wireless Networks," in *Proc of MOBICOM*, 2010.

[20] M. Park, "IEEE 802.11ac : Dynamic Bandwidth Channel Access," in *Proc. of IEEE ICC*, 2011.

[21] L. Cariou and J. Benko, "Multi-channel transmissions," http://mentor.ieee.org/802.11/dcn/09/11-09-1022-00-00 ac-multi-channel-transmissions.ppt.